

---

## Summary

# Development of Curcuminoids based Novel Supramolecular Architectures for Anticancer Drug Delivery Systems

Chemotherapy, usually known as chemo, is a type of cancer therapy that employs drugs to eradicate cancer cells<sup>1</sup>. Chemotherapy attempts to stop tumour growth and cell division in order to prevent invasion and metastasis. Tumour growth can be slowed down at various levels both inside the cell and in its surroundings by chemotherapeutics. Contrary to popular belief, traditional chemotherapy has several downsides. They include poor absorption, large dose requirements, unfavourable side effects, low therapeutic indices, development of multiple drug resistance, and non-specific targeting<sup>2</sup>.

By utilising the differences between the normal cells and tumour microenvironments, such as the different temperatures, ions, pH, and enzyme levels that act as stimulants for drug release, supramolecular chemistry offers the most efficient method of specific release of drugs to the tumour cells<sup>3</sup>. Possibilities of physical, chemical or enzymatic disruptions of the active ingredient are reduced by enclosing the molecules inside a protective shell-like structure. This packaging prevents the drug from degrading and enables it to reach the desired location in the body<sup>4</sup>.

The term "chemistry beyond the molecule" refers to supramolecular chemistry. Supramolecular chemistry, which uses particular, directed, adjustable, and reversible molecular recognition motifs, has been shown to be an effective method for creating regulated and organized materials<sup>5</sup>. These macrocyclic hosts (figure 1) such as crown ethers, cyclodextrins, calixarenes, pillarenes, and cucurbiturils typically include hydrophobic cavities for embedding guest molecules which includes potent cancer-fighting ingredient<sup>6-9</sup>.

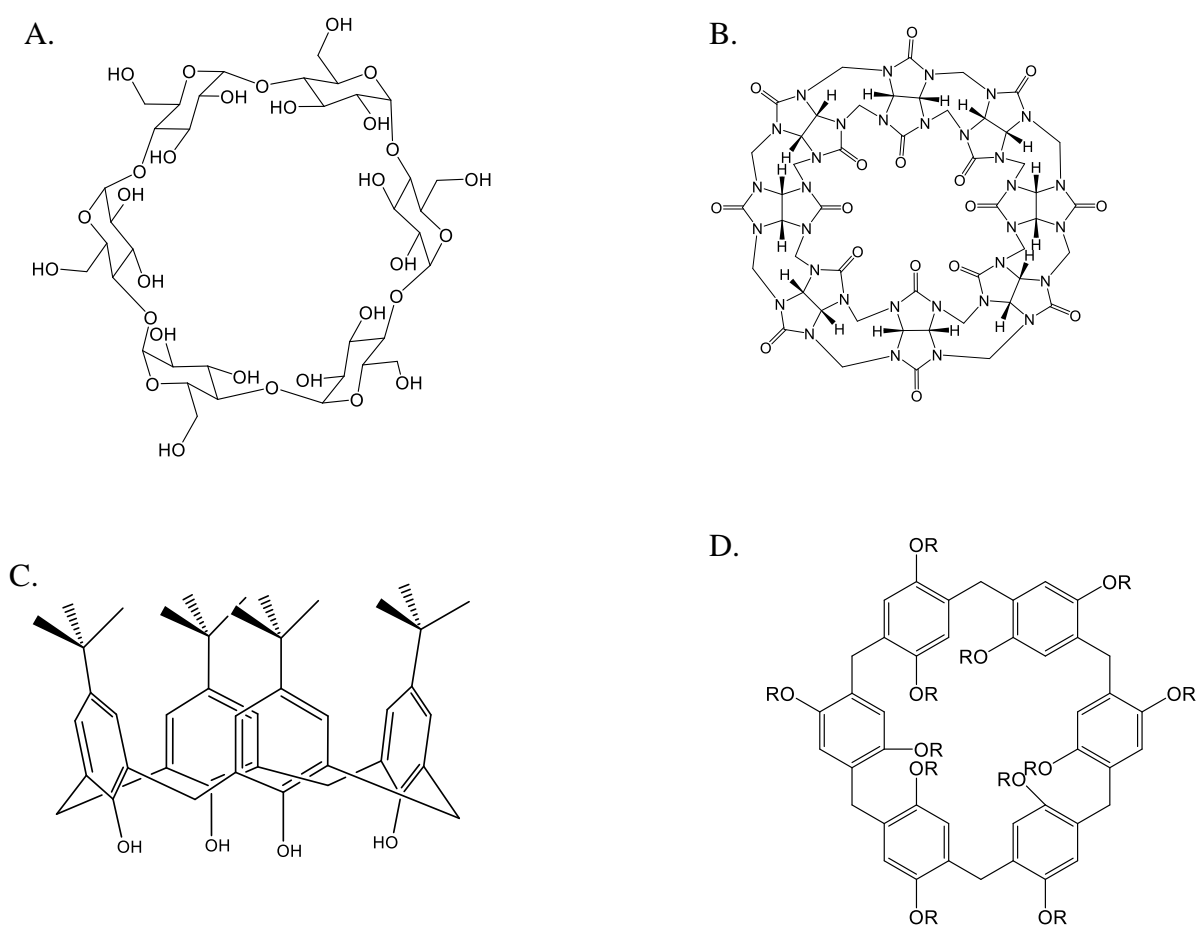


Figure 1. Examples of macrocyclic hosts, A. Cyclodextrin, B. Cucurbituril, C. Calixarene, D. Pillarene.

The supramolecular macrocyclic host can form multifunctional assemblies by complexing various types of guests using its macrocyclic cavity<sup>10</sup>. When compared to the direct administration of bare chemotherapy drugs, drug encapsulation in a carrier offers a number of benefits, including protection from bloodstream drug breakdown, improved solubility, increased stability, targeted drug delivery, a reduction in toxic side effects, and improved pharmacokinetic and pharmacodynamic properties of a drug<sup>11,12</sup>.

The designing of the novel drug delivery system with low toxicity and high therapeutic efficacy, leads the interest to the traditional gold medicine, turmeric. Turmeric (*Curcuma longa* L.), a nutritional dietary spice from the Zingiberaceae family, has been extensively used for various applications<sup>13</sup>. Numerous studies have demonstrated the therapeutic potential of curcumin, including but not limited to its antioxidant, anticarcinogenic, antibacterial, anti-inflammatory, hypoglycemic, hepato- and neuroprotective properties<sup>14-16</sup>. The curcumin

---

molecule has two orthomethoxyphenolic groups joined by a seven-carbon linker chain with a methylene site between two dicarbonyl  $\beta$ -ketone moieties. Depending on the context, the presence of the  $\beta$ -diketo group in chemical structure of curcumin undergoes keto-enol tautomerism<sup>17</sup>. Curcumin is a perfect therapeutic agent due to its cytotoxicity, but its low bioavailability raises serious issues when used in clinical settings<sup>18</sup>.

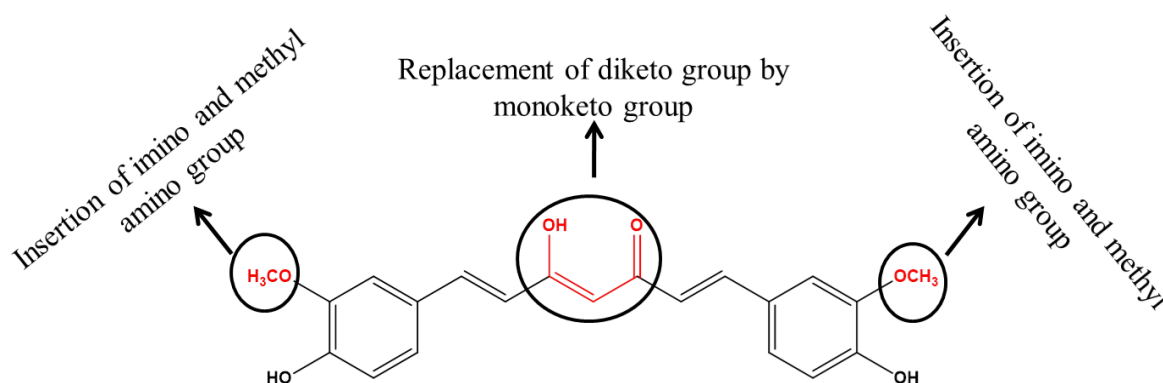


Figure. 2. Proposed modification in the structure of Curcumin to increase its bioavailability and aqueous solubility.

The effectiveness of curcumin was noticeably improved when a  $\beta$ -diketo group<sup>19</sup> was replaced with a monoketo group, such as acetone<sup>20-22</sup>, cyclohexanone<sup>23,24</sup>, cyclopentanone<sup>25</sup> or piperidone<sup>26,27</sup> (Figure 1). Because the ring strain in the cyclopentanone moiety renders bis-hydroxybenzylidene cyclopentanone sterically inappropriate for receptor binding, the bis-hydroxybenzylidene cyclohexanone is known to have a superior efficacy than the cyclopentanone analogues among the cycloalkanone derivatives<sup>28-30</sup> (figure 2).

Being inspired by the research on curcumin over decades which have widely explored the toxicity of curcumin on oncogenic cells, we have designed and synthesized various novel curcuiminoid based drug carriers with the aim to achieve high therapeutic activity.

The thesis divided in six chapters.

**Chapter 1:** It is an introductory chapter which gives brief understanding of supramolecular drug delivery systems.

**Chapter 2:** It comprises of synthesis and characterization of bis-hydroxybenzylidene cyclohexanone, bis-aldehyde and tetraaminochiralcorand. The method employed for the

synthesis of bis-hydroxybenzylidene cyclohexanone was based on stork-enamin reaction which is previously reported. Bis-benzylidene cyclohexanone was further employed for formylation on the ortho position of the –OH group of the phenyl ring without any additional purification (figure 3). The bis-formylation was performed via modified duff formylation reaction and purified by column chromatography. The bis-aldehyde was characterized by various techniques. The single crystal XRD analysis revealed that the dimer of bis-aldehyde is held by intermolecular C-H----- $\pi$  interactions (figure 4).

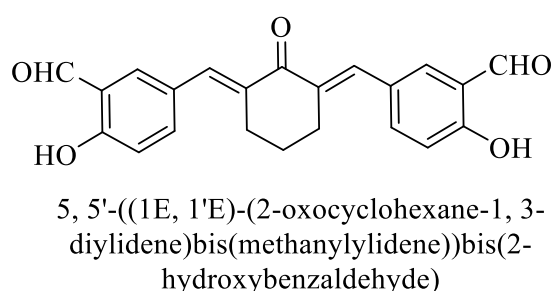


Figure. 3. Structure of bis-aldehyde.

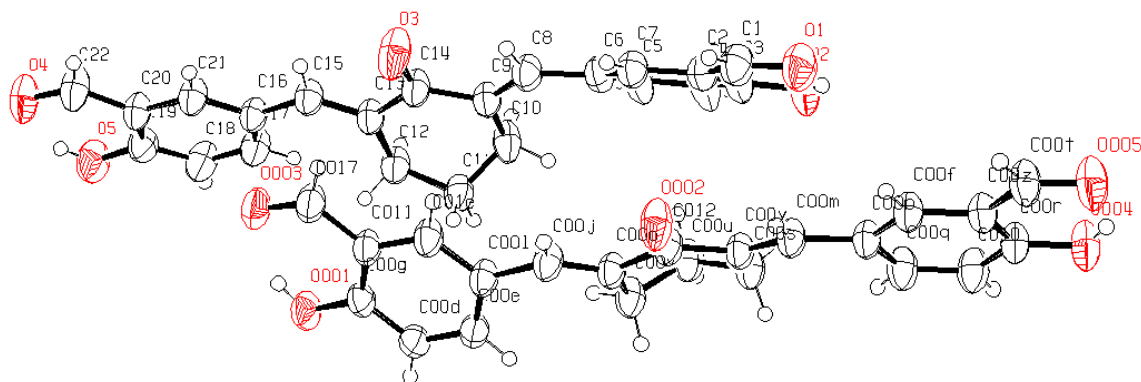


Figure. 4. ORTEP diagram of bis-aldehyde.

The high dilution synthesis was employed to generate the macrocycle, tetraaminochiralcorand from bis-aldehyde and (1*R*, 2*R*)-cyclohexane-1, 2-diamine. The synthesized tetraaminochiralcorand was a cyclocondensed product and was characterized using various spectral techniques. Single crystal XRD analysis revealed the definite cavity with the dimension of 6.890 Å x 18.289 Å of tetraaminochiralcorand (figure 5).

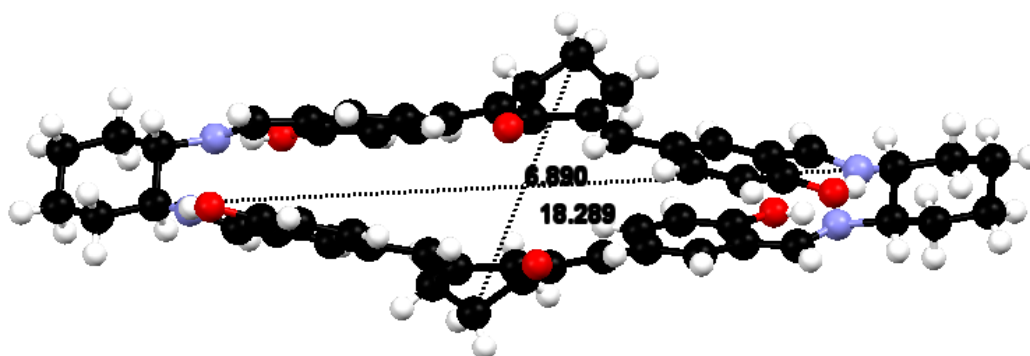


Figure. 5. Intrinsic cavity dimension of Tetraaminochiralcorand.

Utilising the cavity dimension of tetraaminochiralcorand we developed the two combinatorial system: A.  $\text{Ag}^+$  and Nilutamide, B. Cis-platin and Dasatinib. Silver being immunomodulator and drug Nilutamide known to have anticancer properties were encapsulated in a curcuminoid based tetraaminochiralcorand to develop a combinatorial system with pH triggered and sustained drug release capabilities. The MTT assay against MDA-MB-231 cell line revealed the self-therapeutic behavior of tetraaminochiralcorand and found synergistic cytotoxic effect on cancerous cells after loading the drug nilutamide.

In another combinatorial system cis-platin and dasatinib were chosen. Cis-platin is a potent and versatile anticancer drug but cancer cells develop resistance after a period of time. Dasatinib is known to be used with the combination of cis-platin to overcome the resistance of cis-platin. We have encapsulated the combination of drug cis-platin and dasatinib within the tetraaminochiralcorand to achieve a sustained release of drug dasatinib under pH stimulus. The MTT assay against MDA-MB-231 cell line revealed the enhanced cell internalization of drugs when bound with carrier or synergistic cytotoxic effect of carrier on cancerous cells after encapsulating cis-platin and dasatinib.

Both the developed combinatorial system showed the better toxicity on cancerous cell line suggests their potential in chemotherapy.

**Chapter 3:** This chapter comprises the synthesis of cryptand. The high dilution synthesis was employed to generate the desired hexaminocryptand from bis-aldehyde and TREN (Tris-2-aminoethylamine) (figure 6). The hexaminocryptand is a cyclocondensed product and is characterized using various spectral techniques. Single crystal XRD analysis revealed the definite cavity with the dimension of  $19.822 \text{ \AA} \times 7.569 \text{ \AA} \times 4.498 \text{ \AA}$  (figure 7).

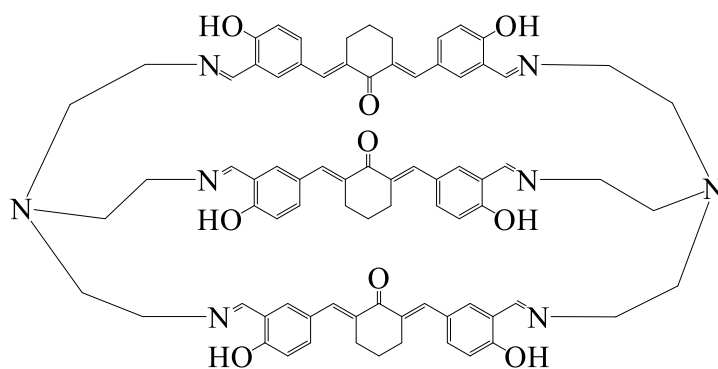


Figure. 6. Structure of Hexaiminiocryptand.

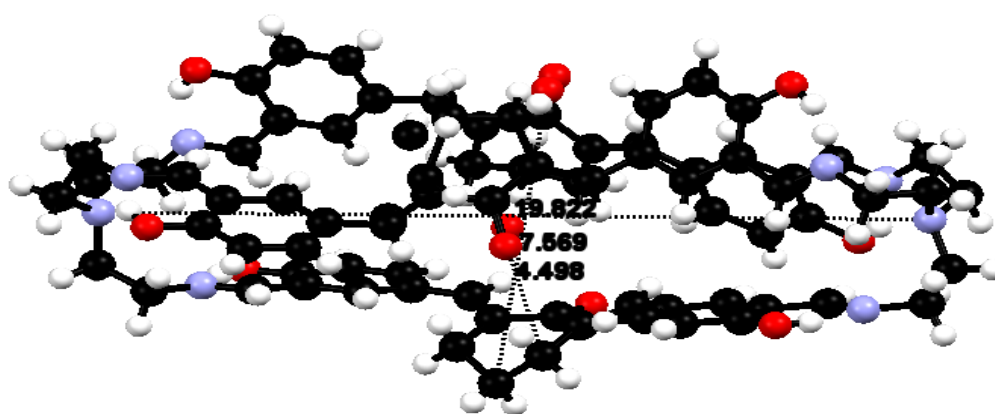


Figure. 7. Intrinsic cavity dimension of hexaiminocryptand.

Further, the selective reduction of hexaiminocryptand by using sodium triacetoxyborohydride takes place which introduces the flexibility to the system (figure 8). The synthesized octaminocryptand is characterized by various spectral techniques.

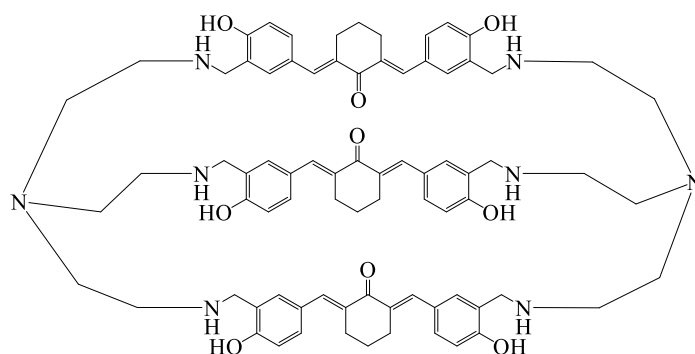


Figure. 8. Structure of Octaminocryptand.

---

The selective reduction of imine bond of hexaiminocryptand gives the flexibility and aqueous solubility to the system. This property of octaminocryptand is helpful in delivery of the BCS class II and III drug which have low aqueous solubility and low permeability<sup>41</sup>. We chose two drugs from the class of BCS II and one drug from BCS class III drug.

Methotrexate, a BCS class II drug was loaded on octaminocryptand to enhances the aqueous solubility with pH triggered and sustained drug release capabilities. The in vivo study revealed the non-toxicity of cryptand on healthy animals. The MTT assay against the MCF-7 and HeLa cell line showed enhanced cell internalization or the synergistic cytotoxic effect of methotrexate on cancerous cells after getting encapsulated with octaminocryptand.

The other drug of BCS class II, flutamide was encapsulated by octaminocryptand to enhances the aqueous solubility with pH triggered and sustained drug release capabilities. The MTT assay against the MDA-MB-231 cell line showed enhanced cytotoxicity of inclusion complex as compared to free drug flutamide.

The BCS class III drug, gemcitabine hydrochloride was encapsulated by octaminocryptand to enhances the aqueous solubility with pH triggered and sustained drug release capabilities. The MTT assay against the MDA-MB-231 cell line showed the enhanced cytotoxicity of inclusion complex as compared to free drug gemcitabine hydrochloride.

**Chapter 4:** This chapter is divided into two parts. First part comprises the synthesis of tetraaminocorand. The high dilution synthesis was employed to generate the desired tetraaminocorand from bis-aldehyde and N<sup>1</sup>- (2-aminoethyl)ethane-1, 2-diamine (figure 9). The synthesis of tetraaminocorand was a cyclocondensed product and characterized using various spectral techniques. Single crystal XRD analysis revealed the definite cavity with the dimension of 6.541 Å x 19.593 Å (figure 10).

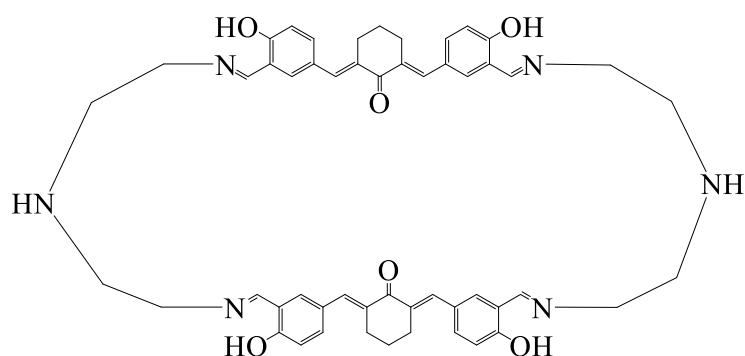


Figure. 9. Structure of Tetraaminocorand.

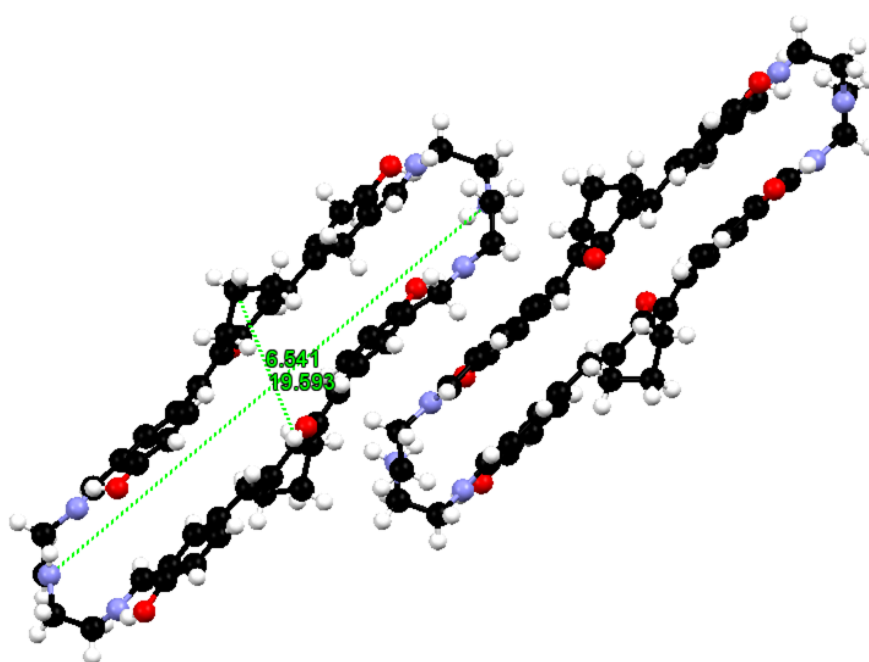


Figure. 10. Intrinsic cavity dimension of Tetraaminocorand.

Further, the tetraaminocorand was loaded with gadolinium to produce the gadolinium corate. Gadolinium corate was loaded with flufenamic acid and further characterized by various spectral techniques. This developed drug carrier showed the pH triggered and sustained drug release capabilities.

The second part of this chapter comprises the reduction of imine bond of tetraaminocorand and formation of vesicle. The selective reduction of imine bonds of tetraaminocorand takes place by using sodiumtriacetoxyborohydride (figure 11). The reduced hexaminocorand further undergo the pegylation with the help of PEG-diacid-600 in order to the formation of

vesicle (figure 12). The vesicle was loaded with capecitabine and showed the pH triggered and sustained drug release of capecitabine.

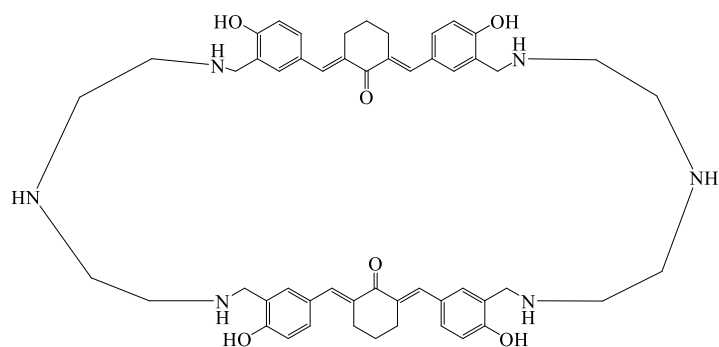


Figure. 11. Structure of Hexaminocorand.

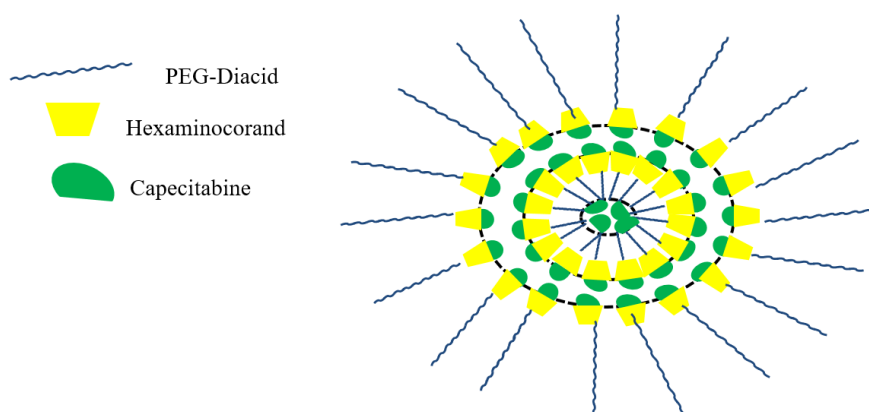


Figure. 12. Proposed structure of Vesicle.

**Chapter 5:** This chapter comprises the synthesis of supramolecular architectures using carbon dots produced from lemon. In first step, the carbon dots from lemon (LCDs) were synthesized by hydrothermal method. In next step, several types of curcuminoids are chosen for creating a supramolecular architecture from LCDs. The said architectures are compared with the architectures formed from bis-demethoxy curcumin and LCDs. For synthesis of these architectures the DCC and DMAP were used, which activated the carboxylic acid groups present on the surface of LCDs. The activated carboxylic acid groups undergo esterification and form a covalent bond with the curcumin and curcuminoid linkers (figure 13).

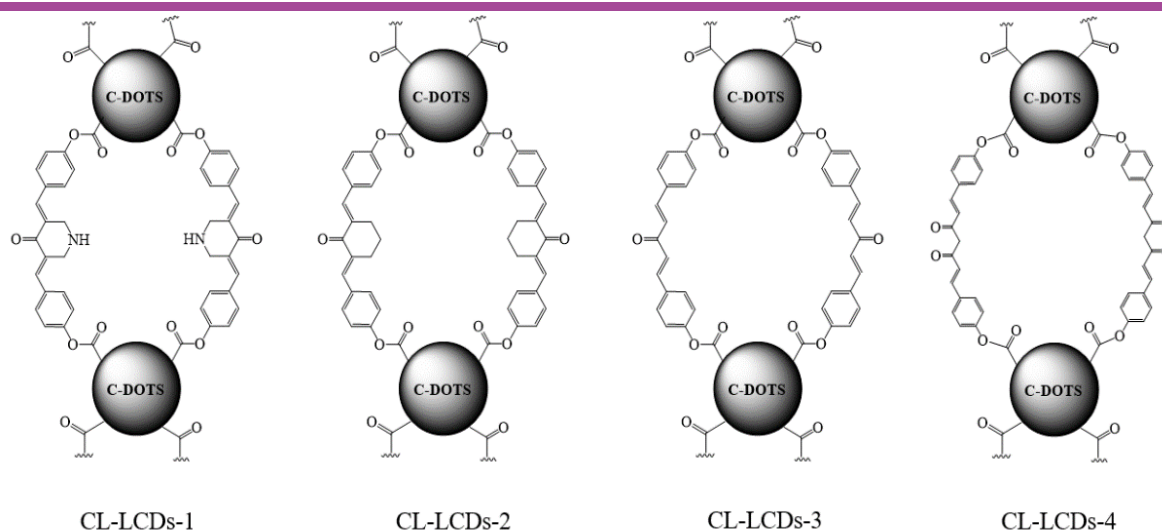


Figure. 13. Various curcuminoid linked lemon carbon dots (CL-LCDs).

In order to explore the drug loading and release profile of synthesized architectures, we loaded the architectures with drug methotrexate. The release profiles of the drug methotrexate loaded on various CL-LCDs demonstrate that the CL-LCD-3 at pH 5.5 exhibits the slowest drug release and highest drug loading capacity amongst all the CL-LCDs. Similar behaviour is seen in CL-LCDs-4, which, when compared to its two other derivatives, CL-LCDs-1 and CL-LCDs-2, exhibits superior loading capacity and sustained release at pH 5.5.

As compared to the standard drug methotrexate, all drug loaded architectures (CL-LCDs) exhibit better toxicity on HeLa cells. They are well tolerated by normal cell lines (HEK293). The CL-LCDs-1 exhibits the highest toxicity on HeLa cells amongst all the CL-LCDs.

**Chapte 6:** The chapter describes the customised synthesis of nanoassemblies based on previously synthesized supramolecular architecture in chapter 5. The synthesis of nanoassembly takes place in three steps. In first step, the lemon based carbon dots (LCDs) were synthesized via hydrothermal method. In second step, triethoxysilylpropan-1-amine was added to the solution of freshly prepared LCDs at room temperature, which causes passivation on the surface of LCDs. In third step, the amine functional group modified LCDs-NH<sub>2</sub> were extracted in n-butanol and condensed with bis-aldehyde to generate nanoassemblies (figure 14).

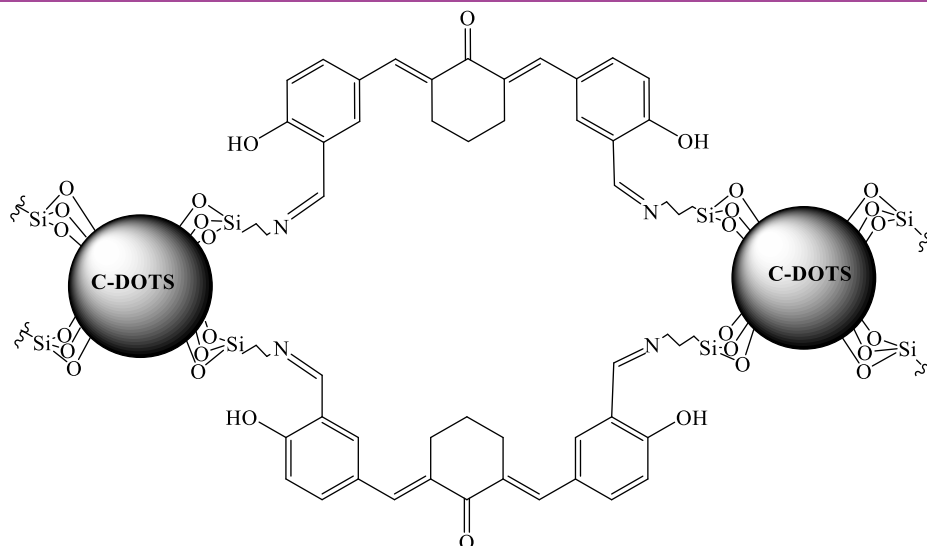


Figure. 14. Structure of nano-assembly.

Due to increase in spacer size and additional imine functionality, the methotrexate loaded LCDs nanoassembly reveals the better entrapment efficiency, enhanced drug loading, and sustained release of methotrexate as compared to CL-LCDs-2.

In comparison to unbound methotrexate, methotrexate-loaded LCDs nanoassemblies exhibit enhanced cytotoxicity towards MCF-7 cancer cell lines.

---

## References:

- 1 A. Alam, U. Farooq, R. Singh, V. P. Dubey, S. Kumar, R. Kumari, K. Kumar, *Open Acc. J. of Toxicol.*, 2018, **2**, 1-6.
- 2 S. Senapati, A. K. Mahanta, S. Kumar, P. Maiti, *Sig. Transduct. Target. Ther.*, 2018, **3**, 1-19.
- 3 J. Kapoor, *J. Nanosci. Nanomed.*, 2022, **6**, 1-3.
- 4 B. Felice, M. P. Prabhakaran, A. P. Rodríguez, S. Ramakrishna, *Mater. Sci. Eng. C*, 2014, **41**, 178-195.
- 5 M. J. Webber, R. Langer, *Chem. Soc. Rev.*, 2017, **46**, 6600-6620.
- 6 G. Yu, K. Jie, F. Huang, *Chem. Rev.*, 2015, **115**, 7240-7303.
- 7 Z. Niu, F. Huang, H. W. Gibson, *J. Am. Chem. Soc.*, 2011, **133**, 2836–2839.
- 8 K. Kim, N. Selvapalam, Y. H. Ko, K. M. Park, D. Kim, J. Kim, *Chem. Soc. Rev.*, 2007, **36**, 267–279.
- 9 E. A. Appel, J. D. Barrio, X. J. Loh, O. A. Scherman, *Chem. Soc. Rev.*, 2012, **41**, 6195-6214.
- 10 P. Chen, B. Shi, *Prog. Chem.*, 2017, **29**, 720-739.
- 11 H. Maeda, J. Wu, T. Sawa, Y. Matsumura, K. Hori, *J. Control. Release*, 2000, **65**, 271-284.
- 12 H. Koo, M. S. Huh, I. C. Sun, S. H. Yuk, K. Choi, K. Kim, I. C. Kwon, *Acc. Chem. Res.*, 2011, **44**, 1018-1028 .
- 13 P. Anand, C. Sundaram, S. Jhurani, A. B. Kunnumakkara, B. B. Aggarwal, *Cancer Lett.*, 2008, **267**, 133–164.
- 14 B. Joe, M. Vijaykumar, B. R. Lokesh, *Crit. Rev. Food Sci. Nutr.*, 2004, **44**, 97–111.
- 15 S. J. Hewlings, D. S. Kalman, *Foods*, 2017, **6**, 1–11.
- 16 S. Heidari, S. Mahdiani, M. Hashemi, F. Kalalinia, *Biotechnol. Appl. Biochem.*, 2020, **67**, 430–441.

- 
- 17 F. C. Rodrigues, N. V. Anil Kumar, G. Thakur, *Eur. J. Med. Chem.*, 2019, **177**, 76–104.
  - 18 P. Vitaglione, R. Barone Lumaga, R. Ferracane, I. Radetsky, I. Mennella, R. Schettino, S. Koder, E. Shimoni, V. Fogliano, *J. Agric. Food Chem.*, 2012, **60**, 3357–3366.
  - 19 S. Omid, A. Kakanejadifard, *RSC Adv.*, 2020, **10**, 30186–30202.
  - 20 M. A. Tomeh, R. Hadianamrei, X. Zhao, *Int. J. Mol. Sci.*, 2019, **20**, 1-26.
  - 21 L. Friedman, L. Lin, S. Ball, T. Bekaii-Saab, J. Fuchs, P. K. Li, C. Li, J. Lin, *Anticancer Drugs*, 2009, **20**, 444–449.
  - 22 L. Lin, B. Hutzen, S. Ball, E. Foust, M. Sobo, S. Deangelis, B. Pandit, L. Friedman, C. Li, P. K. Li, J. Fuchs, J. Lin, *Cancer Sci.*, 2009, **100**, 1719–1727.
  - 23 J. R. Fuchs, B. Pandit, D. Bhasin, J. P. Etter, N. Regan, D. Abdelhamid, C. Li, J. Lin, P. K. Li, *Bioorganic Med. Chem. Lett.*, 2009, **19**, 2065–2069.
  - 24 S. Mapoung, S. Suzuki, S. Fuji, A. Naiki-Ito, H. Kato, S. Yodkeeree, C. Ovatlarnporn, S. Takahashi, P. Limtrakul, *Cancer Sci.*, 2019, **110**, 596–607.
  - 25 H. Ohori, H. Yamakoshi, M. Tomizawa, M. Shibuya, Y. Kakudo, A. Takahashi, S. Takahashi, S. Kato, T. Suzuki, C. Ishioka, Y. Iwabuchi, H. Shibata, *Mol. Cancer Ther.*, 2006, **5**, 2563–2571.
  - 26 I. Huber, E. Pandur, K. Sipos, L. Barna, A. Harazin, M. A. Deli, L. Tyukodi, G. Gulyás-Fekete, G. Kulcsar, Z. Rozmer, *Eur. J. Pharm. Sci.*, 2022, **173**, 106184.
  - 27 A. Thakur, S. Manohar, C. E. Velez Gerena, B. Zayas, V. Kumar, S. V. Malhotra, D. S. Rawat, *Med. chem. comm.*, 2014, **5**, 576–586.
  - 28 S. N. H. Zamrus, M. N. Akhtar, S. K. Yeap, C. K. Quah, W. S. Loh, N. B. Alitheen, S. Zareen, S. N. Tajuddin, Y. Hussin, S. A. A. Shah, *Chem. Cent. J.*, 2018, **12**, 1–10.
  - 29 H. Itokawa, Q. Shi, T. Akiyama, S. L. Morris-Natschke, K. H. Lee, *Chin. Med.*, 2008, **3**, 1–13
  - 30 P. Mathur, M. Mori, H. Vyas, K. Mor, J. Jagtap, S. Vadher, K. Vyas, R. Devkar, A. Desai, *ACS Omega*, 2022, **7**, 45545–45555.